J. Fluid Mech. (1996), *vol.* 315, *pp.* 119–137

Receptivity of pipe Poiseuille flow

By ANATOLI TUMIN

Department of Fluid Mechanics and Heat Transfer, Tel-Aviv University, Tel-Aviv 69978, Israel

(Received 3 February 1995 and in revised form 29 November 1995)

The receptivity problem is considered for pipe flow with periodic blow–suction through a narrow gap in the pipe wall. Axisymmetric and non-axisymmetric modes (1, 2, and 3) are analysed. The method of solution is based on global eigenvalue analysis for spatially growing disturbances in circular pipe Poiseuille flow. The numerical procedure is formulated in terms of the collocation method with the Chebyshev polynomials application. The receptivity problem is solved with an expansion of the solution in a biorthogonal eigenfunction system, and it was found that there is an excitation of many eigenmodes, which should be taken into account. The result explains the non-similar character of the amplitude distribution in the downstream direction that was observed in experiments.

1. Introduction

Reynolds (1883) discovered that a laminar pipe flow becomes a turbulent one when the Reynolds number is large enough. Although numerous theoretical and experimental investigations of pipe flow have been carried out, the nature of the transition process is not yet understood.

Analytical and numerical methods in theoretical studies of flow stability have been used. The classic hydrodynamic stability theory (Lin 1955; Drazin & Reid 1981) deals with so-called normal mode analysis. It means, in an example with axisymmetric disturbances, that disturbance of the stream function is given by

$$\Psi = \Phi(r)\exp(\mathrm{i}\alpha z - \mathrm{i}\omega t), \tag{1.1}$$

where α is a wavenumber, ω is a frequency. The amplitude function Φ satisfies an ordinary differential equation with boundary conditions, and a relation between α and ω is determined from the boundary value problem. There are two approaches: the temporal and the spatial stability theories. According to the temporal theory, the disturbance is considered as growing with respect to time. The wavenumber α is a real parameter and the frequency ω is a complex one. The disturbance grows when $\mathrm{Im}(\omega) > 0$. In the spatial stability theory, the disturbance is considered as growing in the downstream direction. The frequency ω is a real parameter and the wavenumber α is a complex one. The downstream propagating disturbances grow if $\mathrm{Im}(\alpha) < 0$. The classic hydrodynamic stability theory assumes that the existence of a normal mode growing in the downstream direction means instability of the flow. The theory explains a laminar–turbulent transition as being caused by amplification of the mode.

Almost all the theoretical results concerning the linear stability of pipe Poiseuille flow have been obtained by using the temporal theory. We refer to the studies of Sexl (1927 *a,b*), Pretsch (1941), Pekeris (1948), Corcos & Sellars (1959), Lessen, Sadler

& Liu (1968), and Salwen & Grosch (1972), and Salwen, Cotton & Grosch (1980). The spatial stability was investigated by Gill (1965) analytically and by Garg & Rouleau (1972) numerically (a special case of the spatial theory with stationary disturbances was published by Bramley 1986). The theoretical results showed that a parabolic velocity profile is stable with respect to axisymmetric and non-axisymmetric infinitesimal disturbances.

Owing to the failure to find an instability of a parabolic velocity profile, it was suggested that the laminar–turbulent transition could be explained by a particularity of a flow at the inlet (Tatsumi 1952). The important role of flow development at the inlet was proved in the experiment by Wygnanski & Champagne (1973). Based on these results, Morkovin & Reshotko (1989) formulated in their review: "Experimenters agree that the most likely bypasses are to be found in the linearly weakly unstable slowly accelerating boundary layers before parabolic flow is fully developed."

Earlier, Fox, Lessen & Bhat (1968) found in their experiment that disturbances may grow in fully developed pipe flow, but for a long time their results have been considered as unreliable. Recently, Darbyshire & Mullin (1995) established that there is a critical amplitude of disturbances that causes transition to turbulence, and that this amplitude depends on the Reynolds number. The experimental results qualitatively agree with the numerical modelling of onset of turbulence (Boberg & Brosa 1988). Probably, there is a strong nonlinear mechanism of transition to turbulence in fully developed pipe flow.

Nevertheless, new ideas have been proposed in order to determine the growth of small disturbances in circular laminar pipe flow. Gustavsson (1989) considered the possibility of direct resonance between pressure eigenmodes and streamwise velocity components. Since certain eigenvalues obtained from the equation for pressure disturbance may coincide with eigenvalues of the uniform equation for streamwise velocity disturbance, an algebraic growth may occur at the initial stage of disturbance development. A more general mechanism of transient growth was investigated by Bergström (1992). The results for optimal transient growth in pipe Poiseuille flow were published by Bergström (1993*a*) and Schmid & Henningson (1994). To establish the possibility of the existence of corresponding initial data in a real experiment, a physical model of disturbance excitation should be considered.

In our opinion, there are not yet sufficient experimental investigations of developed pipe flow at the linear stage. The experiments with axisymmetric disturbances induced artificially in the developed part of pipe flow (Leite 1959; Reshotko 1958; Kaskel 1961) showed that the disturbances decay in the downstream direction, but the adequacy of the observed experimental data in the linear theoretical model has not been proved. Leite (1959) observed that the radial distribution of disturbance amplitude depends on downstream distance. In this case, it is not clear which kind of disturbance may be excited in experiments; thus a receptivity problem should be solved for the experiment in order to analyse results. Recently, Bergström (1993*b*) investigated experimentally the evolution of the localized disturbance in a pipe flow. In this case it is also unknown which kind of disturbance is excited, so the receptivity problem should be solved in order to interpret the results.

The receptivity problem is the problem of determining the normal mode amplitude under the influence of an external force on a flow. Morkovin (1969) and Reshotko (1976) clarified an important role of the receptivity problem in a

laminar–turbulent transition process. The formulation of the problem resulted in intensive investigations of various mechanisms responsible for unstable wave excitation. The first theoretical result was obtained by Gaster (1965) for the normal mode generation as a result of a localized forcing at the bottom of a two-dimensional boundary layer; but extensive consideration of the receptivity problem was begun only at the end of the 1970s. At present, we have a vast bibliography on this subject (Zhigulev & Tumin 1987; Goldstein & Hultgren, 1989; Choudhary 1993). Publications covering theoretical models may be categorized according to their underlying principles as follows: (i) the asymptotical analysis of the linearized Navier–Stokes equations with the Reynolds number tending to infinity; (ii) the direct numerical simulation; (iii) the numerical methods based on expansion of a solution in spatial eigenfunctions of the linear stability problem.

Tumin & Fedorov (1984) analysed the receptivity problem with a localized disturbance at the bottom of a two-dimensional incompressible boundary layer flow. The problem of a compressible boundary layer was considered by Fedorov (1984). Their method of solution is based on expansion of the linearized Navier–Stokes equation solutions in a biorthogonal system of eigenfunctions. This method has provided a convenient algorithm of normal mode amplitude calculation for various external forces. Nevertheless, there was an obstacle to extending this method to the supercritical frequencies when an exponential growth in the downstream direction exists; so some additional suggestions had to be made in order to choose a contour in the Fourier–Laplace transform inversion. Ashpis & Reshotko (1990) solved the problem of the correct transform inversion. Their result allows one to establish an inversion contour deformation for the supercritical frequencies and provides a basis for application of the biorthogonal technique. In a pipe flow, no difficulty in the Fourier transform inversion exists since there is no eigenmode which becomes unstable in a band of frequencies; therefore, the biorthogonal eigenfunction technique is especially convenient for the numerical analysis.

The object of the present paper is to consider the receptivity problem for a pipe flow with axisymmetric and non-axisymmetric disturbances forced by a localized periodic blow-suction through a narrow gap in a wall. As a result, we hope to understand qualitative features of disturbances that may be observed in a real experiment.

Briefly, the structure of the paper is as follows. The eigenvalue problem is formulated in § 2.1. The numerical results for axisymmetric and non-axisymmetric disturbances are presented in § 2.2. The receptivity problem is formulated in § 3.1. In § 3.2 the biorthogonal eigenfunction system is introduced. The problem solution is proposed in § 3.3, and numerical results are described in § 3.4. The summary of the paper is given in § 4. In Appendix A we present the matrices used in the analysis. The boundary conditions for the numerical treatment of the adjoint problem are discussed in Appendix B.

2. Eigenvalue problem for circular pipe Poiseuille flow

2.1. *Formulation of the problem for spatially growing disturbances*

Since we are going to consider the receptivity problem as the boundary value problem with a prescribed frequency, we expect that the solution will be obtained as a sum of spatial normal modes. Thus, we begin our analysis with the eigenvalue problem for a pipe flow by using the spatial theory.

We consider a laminar incompressible flow in a circular pipe. The linearized Navier–Stokes equations for radial, tangential and axial velocities u, v, w and pressure disturbance p are written in the cylindrical-polar coordinates (r, θ, z) as

$$\frac{1}{r}\frac{\partial ru}{\partial r} + \frac{1}{r}\frac{\partial v}{\partial \theta} + \frac{\partial w}{\partial z} = 0, \tag{2.1}$$

$$\frac{\partial u}{\partial t} + W\frac{\partial u}{\partial z} = -\frac{\partial p}{\partial r} + \frac{1}{Re}\left(\nabla^2 u - \frac{u}{r^2} - \frac{2}{r^2}\frac{\partial v}{\partial \theta}\right), \tag{2.2}$$

$$\frac{\partial v}{\partial t} + W\frac{\partial v}{\partial z} = -\frac{1}{r}\frac{\partial p}{\partial \theta} + \frac{1}{Re}\left(\nabla^2 v - \frac{v}{r^2} + \frac{2}{r^2}\frac{\partial u}{\partial \theta}\right), \tag{2.3}$$

$$\frac{\partial w}{\partial t} + u\frac{dW}{dr} + W\frac{\partial w}{\partial z} = -\frac{\partial p}{\partial z} + \frac{1}{Re}\nabla^2 w, \tag{2.4}$$

where

$$\nabla^2 \equiv \frac{\partial^2}{\partial r^2} + \frac{1}{r}\frac{\partial}{\partial r} + \frac{1}{r^2}\frac{\partial^2}{\partial \theta^2} + \frac{\partial^2}{\partial z^2}, \tag{2.5}$$

$$W(r) = 1 - r^2. \tag{2.6}$$

We use the following reference scales: centreline velocity W_{max} and radius of the pipe a. Pressure is normalized by $\varrho {W_{max}}^2$ and the Reynolds number is defined as $Re = aW_{max}/\nu$. The disturbances u, v, w, p are assumed in the form:

$$(u(t,r,\theta,z), v(t,r,\theta,z), w(t,r,\theta,z), p(t,r,\theta,z)) = (\hat{u}(r,z), \hat{v}(r,z), \hat{w}(r,z), \hat{p}(r,z))e^{i(n\theta - \omega t)}, \tag{2.7}$$

where parameter n is an integer azimuthal index. We introduce the column vector $\boldsymbol{A}$ with six elements: $A_1 = \hat{u}$; $A_2 = \partial\hat{u}/\partial z$; $A_3 = \hat{w}$; $A_4 = \hat{p}$; $A_5 = \hat{v}$; $A_6 = \partial\hat{v}/\partial z$. Substituting (2.7) into (2.1)–(2.4), we obtain the following system of equations:

$$\frac{\partial \boldsymbol{A}}{\partial z} = \boldsymbol{H}_1\boldsymbol{A} + \boldsymbol{H}_2\frac{\partial \boldsymbol{A}}{\partial r} + \boldsymbol{H}_3\frac{\partial^2 \boldsymbol{A}}{\partial r^2}, \tag{2.8}$$

where $\boldsymbol{H}_1, \boldsymbol{H}_2$ and $\boldsymbol{H}_3$ are 6×6 matrices. The non-zero elements of these matrices are presented in Appendix A. The fourth equation in the system (2.8) is the z-momentum equation where the derivative $\partial^2 w/\partial z^2$ was substituted by the derivative obtained from the continuity equation.

In the spatial theory of hydrodynamic stability, the frequency ω is considered as a real value and solution of the system (2.8) is assumed to be of the form:

$$\boldsymbol{A}(r,z) = \boldsymbol{A}_\alpha(r)e^{i\alpha z}. \tag{2.9}$$

The eigenvector $\boldsymbol{A}_\alpha(r)$ satisfies the following system of ordinary differential equations:

$$i\alpha\boldsymbol{A}_\alpha = \boldsymbol{H}_1\boldsymbol{A}_\alpha + \boldsymbol{H}_2\frac{d\boldsymbol{A}_\alpha}{dr} + \boldsymbol{H}_3\frac{d^2\boldsymbol{A}_\alpha}{dr^2}. \tag{2.10}$$

On a wall, the no-slip condition is assumed for the velocity components:

$$r = 1: \quad A_{1\alpha} = A_{3\alpha} = A_{5\alpha} = 0. \tag{2.11}$$

Owing to the definition of the second and sixth components of the vector $\boldsymbol{A}$, we obtain on a wall:

$$r = 1: \quad A_{2\alpha} = A_{6\alpha} = 0. \tag{2.12}$$

When $r \to 0$, a special consideration is required for the numerical procedure to obtain a finite solution for the centreline. Khorrami, Malik & Ash (1989) formulated the

	Re(α)	Im(α)	
$n = 0$	0.51998925173	0.02083549388	Garg & Rouleau (1972)
	0.51998925171	0.02083549388	Khorrami *et al.* (1989)
	0.51998925173	0.02083549388	Present method ($N = 60$)
	0.51998925173	0.02083549388	Present method ($N = 120$)
$n = 1$	0.5352510831	0.0172276439	Garg & Rouleau (1972)
	0.53525108	0.01722763	Khorrami *et al.* (1989)
	0.5352510831	0.0172276439	Present method ($N = 60$)
	0.5352510831	0.0172276439	Present method ($N = 120$)

TABLE 1. Eigenvalues for the least-stable modes $n = 0$, $n = 1$. $Re = 10000$; $\omega = 0.5$.

boundary conditions as

$$n = 0; r \to 0: \quad A_{1\alpha} = A_{2\alpha} = A'_{3\alpha} = A_{5\alpha} = A_{6\alpha} = 0; \tag{2.13}$$

$$n = \pm 1; r \to 0: \quad -\mathrm{i}A_{1\alpha} \pm A_{5\alpha} = 0; \quad -\mathrm{i}A_{2\alpha} \pm A_{6\alpha} = 0, \tag{2.14}$$

$$A_3 = A_4 = 0, \qquad -2\mathrm{i}A'_1 \pm A'_5 = 0; \tag{2.15}$$

$$|n| > 1; r \to 0: \quad A_{1\alpha} = A_{2\alpha} = A_{3\alpha} = A_{4\alpha} = A_{5\alpha} = 0. \tag{2.16}$$

The numerical method was formulated in terms of the Chebyshev collocation approximation in the form suggested by Khorrami *et al.* (1989). The spectral technique has been applied according to Liang & Reshotko (1991).

To determine the number $(N+1)$ of Chebyshev polynomials in the approximations, we compared the eigenvalues when $N = 60$ and 120. The results obtained show that we can choose $N = 60$ for the first few tens of eigenmodes. The closer to the real axis of α, the better the accuracy.

Comparison of the eigenvalues for the least-stable modes $n = 0$ and $n = 1$ at $R = 10000$ and $\omega = 0.5$ with the results published by Garg & Rouleau (1972) and Khorrami *et al.* (1989) is presented in table 1.

2.2. *Numerical results*

2.2.1. *Azimuthal index 0*

The following results were obtained for the Reynolds number 2280 and frequency $\omega = 0.96$.

In the spectral method, some spurious eigenvalues may occur, thus it is necessary to look out for their occurrence. It is possible to find eigenvalues with the pressure gradient equal to zero in the collocation points and not equal to zero at a boundary. These are so-called pressure spurious modes that should be treated in a special way (Phillips & Roberts 1993). In the present work, the pressure derivative $\mathrm{d}A_{\alpha 4}/\mathrm{d}r$ was calculated for each eigenmode in order to find a spurious eigenvalue. The spurious eigenvalues with azimuthal index 0 are shown in figure 1. There is a set of eigenvalues when $\mathrm{Im}(\alpha) < 0$. The eigenvalues are pure complex at the limit $Re \to \infty$. For $n = 0$ they correspond to the roots of the Bessel function of the first order and the first kind: $\alpha = \pm \mathrm{i}\mu_s; J_1(\mu_s) = 0$ $(s =, 1, 2, ...)$. These eigenvalues were found in the asymptotic analysis by Gill (1965). They do not cross the real axis when the frequency is changed. Equally, this does not mean an instability of a flow. Occurrence of the mode is typical for spatial disturbances which are associated with an impact in the upstream direction.

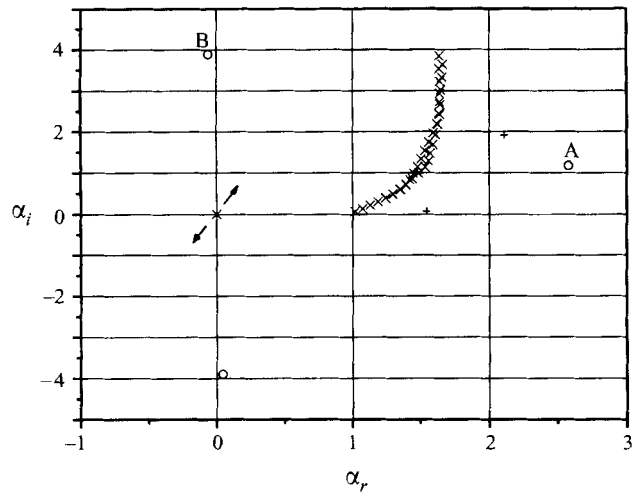

FIGURE 1. Eigenvalues in the complex plane α at $n = 0$. + – spurious pressure eigenmodes. The arrows show the split directions of the 'acoustic' mode.

For the purpose of subsequent data presentation, we label two eigenvalues A and B. Eigenvalue A is apart from the main group of eigenvalues, as is eigenvalue B, which does not belong to the main group but represents a set of eigenvalues close to the imaginary axis.

There are two eigenvalues that are very close to the point $\alpha = 0$. The negligible distinction between them can be explained by the accuracy of the numerical procedure. These eigenvalues correspond to an incompressible limit of the acoustic waves ($\alpha = 0$) spreading in the upstream and downstream directions. To distinguish the 'acoustic' modes, we considered a slightly compressible isothermal gas. In (2.1), an additional term $M^2\partial p/\partial t$ occurs, where parameter M is the Mach number. In figure 1, the arrows show the split directions of the eigenvalues when the Mach number increases. Calculations with $M = 10^{-3}, 10^{-4}$ showed that other eigenmodes were not susceptible to the effect. At the same time, the acoustic mode could be considered numerically. In the acoustic mode, $\alpha \approx \omega M$ and $p \approx w/M$ in most of a flow, as it must for acoustic waves.

The eigenvalues for the first, least-stable eigenmodes are given in the table 2. The eigenvalues are written in the same format as the results for $N = 60$ and $N = 120$. There are two families: torsional and meridional modes. The torsional modes have u, w, p equal to zero and the circumferential velocity component v is not equal to zero. The meridional modes are opposite: $v = 0$ and the other velocity components and the pressure disturbance are not equal to zero. The eigenvalues of these two families are very close. The longitudinal velocity component of the least-stable meridional eigenmode is shown in figure 2.

2.2.2. *Azimuthal indices 1, 2 and 3*

The numerical results for $n = 1, 2$ and 3 are presented in table 3. The results are the same for $N = 60$ and $N = 120$. The character of the eigenvalue location in the complex plane α when $n = 1$ is shown in figure 3. The eigenvalue maps for $n = 2$ and 3 are similar. In figure 3 we distinguish two neighbouring groups of eigenvalues (denoted as 1 and 2), and label the distant eigenvalues A,B,C and D. In principle, the eigenvalue C represents the eigenvalues along the imaginary axis.

Number of eigenmode	Re(α)	Im(α)	Type of eigenmode
1	1.0179142	0.6206459×10^{-1}	M1
2	1.0179143	0.6206472×10^{-1}	T1
3	1.0754886	0.13105881	M2
4	1.0754915	0.13105898	T2
5	1.1324143	0.20770561	T3
6	1.1323954	0.20772219	M3
7	1.1883721	0.29232825	T4
8	1.1883601	0.29247350	M4
9	1.2430636	0.38525837	T5
10	1.2434624	0.38575800	M5
11	1.2962040	0.48683492	T6
12	1.2984931	0.48716030	M6
13	1.3530214	0.5928706	M7
14	1.3475094	0.5973831	T7

TABLE 2. Eigenvalues for the first, least-stable eigenmodes, $n = 0$. $Re = 2280$; $\omega = 0.96$. M – meridional eigenmode; T – torsional eigenmode.

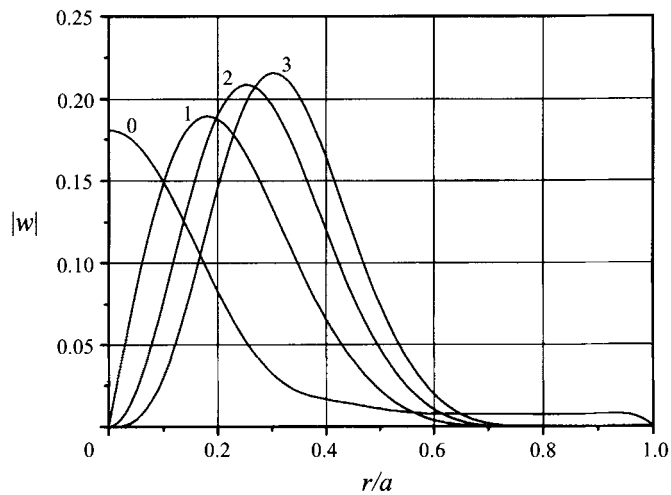

FIGURE 2. Eigenfunctions of the least-stable modes $n = 0, 1, 2, 3$; longitudinal velocity component.

We have not found spurious eigenvalues among the disturbances of the modes considered. The first eigenfunctions are shown in figure 2.

3. The receptivity problem in pipe flow

3.1. *Formulation of the problem*

Let us consider a laminar flow in a circular pipe with a periodic blow–suction forcing the flow through a slot. It is necessary to determine disturbance behaviour in the pipe downstream from the slot. We suggest that the forcing amplitude is sufficiently small and we may use the system (2.8) for the disturbance with a prescribed frequency. Only one harmonic with respect to time t and angle ϑ is considered. Thus, the

Number of eigenmode	$n=1$		Family of eigenmode ($n=1$)	$n=2$		$n=3$		Family of eigenmode ($n=2,3$)
	Re(α)	Im(α)		Re(α)	Im(α)	Re(α)	Im(α)	
1	1.0635965	0.5122505×10^{-1}	1	1.091291	0.7696552×10^{-1}	1.119773	0.10921440	1
2	1.0029119	0.10410148	2	1.0217890	0.13485084	1.045175	0.16798574	2
3	1.1321799	0.11728354	1	1.1580435	0.14749418	1.1852898	0.18413389	1
4	1.0521692	0.1793126	2	1.0710396	0.2125134	1.094342	0.24835630	2
5	1.1997767	0.1923576	1	1.2235639	0.22684628	1.2496671	0.26785190	1
6	1.101562	0.2601731	2	1.119770	0.29668867	1.142572	0.33579408	2
7	1.267542	0.2763042	1	1.2881320	0.31497875	1.312932	0.36048367	1
8	1.1504159	0.34804764	2	1.1674405	0.38829801	1.1894143	0.43099097	2
9	1.3366018	0.37010973	1	1.351907	0.4122068	1.375158	0.4623577	1
10	1.5592829	0.44034987	A	1.2136651	0.4879833	1.2345223	0.53449396	2
11	1.1983124	0.4437593	2	1.4156198	0.5191714	1.4369407	0.57373813	1
12	1.4077545	0.47947440	1	1.2581277	0.59625491	1.277596	0.6467463	2
13	1.2449138	0.5479323	2	1.4822959	0.63631208	1.4998787	0.69353671	1
14	1.466419	0.61187152	1	1.3004755	0.71352031	1.3182548	0.76810573	2

TABLE 3. Numerical results for $n = 1, 2$ and 3. $Re = 2280$; $\omega = 0.96$.

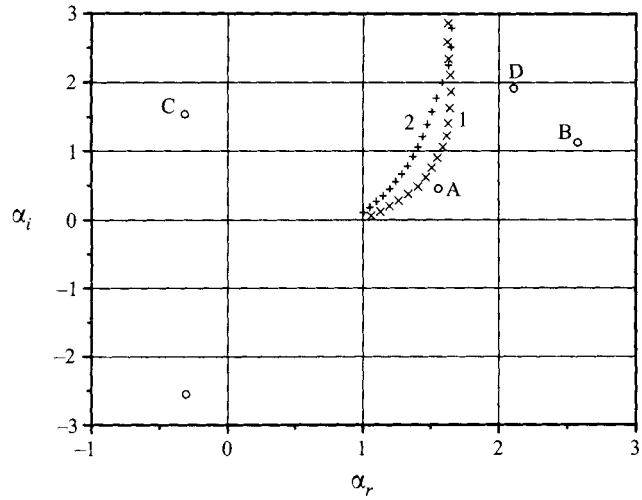

FIGURE 3. Eigenvalues in the complex plane α at $n = 1$.

solution is assumed to be in a form $\propto \exp(in\vartheta - i\omega t)$. For the harmonic, the boundary conditions imitating the periodic blow-suction through a narrow slot of width d, have the following form:

$$\left.\begin{array}{lll} r = 1: & u = 0, & |z| > d/2; \\ & u = f(z), & |z| < d/2; \\ & w = 0; & \\ & v = 0; & \end{array}\right\} \tag{3.1}$$

where $f(z)$ is the shape function of the velocity disturbance on the wall.

We assume that disturbances decay in the downstream and upstream directions, so the problem can be solved by using the Fourier transform

$$\Phi(r;\alpha_v) = \int_{-\infty}^{\infty} \phi(r;z)\,\mathrm{e}^{-\mathrm{i}\alpha_v z}\mathrm{d}z. \tag{3.2}$$

From (2.8) we obtain a system of ordinary differential equations that is written in the form

$$\mathrm{i}\alpha_v \boldsymbol{A}_v = \boldsymbol{H}_1 \boldsymbol{A}_v + \boldsymbol{H}_2 \frac{\mathrm{d}\boldsymbol{A}_v}{\mathrm{d}r} + \boldsymbol{H}_3 \frac{\mathrm{d}^2 \boldsymbol{A}_v}{\mathrm{d}r^2}. \tag{3.3}$$

We write the boundary conditions on the wall as

$$\left.\begin{array}{ll} r = 1: & A_{v1} = \varrho(\alpha_v); \\ & A_{v3} = 0; \\ & A_{v5} = 0; \end{array}\right\} \tag{3.4}$$

where

$$\varrho(\alpha_v) = \int_{-\infty}^{\infty} f(z)\mathrm{e}^{-\mathrm{i}\alpha_v z}\mathrm{d}z. \tag{3.5}$$

The solution of the system (3.3) at the centreline must be finite; this restriction may be written as in (2.13)–(2.16).

After solving the problem in terms of $\boldsymbol{A}_v$, we obtain the solution in the physical

domain as the integral

$$\boldsymbol{A}(r;z) = \frac{1}{2\pi}\int_{-\infty}^{\infty} \boldsymbol{A}_v(r;\alpha_v)\,\mathrm{e}^{\mathrm{i}\alpha_v z}\,\mathrm{d}\alpha_v. \tag{3.6}$$

The main difficulties are associated with evaluation of the integral in (3.6). To analyse the behaviour of the solution at some distance from the slot, it would be useful to develop an appropriate procedure to present the solution as a sum of the normal modes with known amplitudes.

3.2. *Biorthogonal eigenfunction system*

We introduce the following biorthogonal system of eigenfunctions $\{\boldsymbol{A}_\alpha, \boldsymbol{B}_\alpha\}$:

$$\mathrm{i}\alpha\boldsymbol{A}_\alpha = \boldsymbol{H}_1\boldsymbol{A}_\alpha + \boldsymbol{H}_2\frac{\mathrm{d}\boldsymbol{A}_\alpha}{\mathrm{d}r} + \boldsymbol{H}_3\frac{\mathrm{d}^2\boldsymbol{A}_\alpha}{\mathrm{d}r^2}; \tag{3.7}$$

$$r = 1: \qquad A_{\alpha 1} = A_{\alpha 3} = A_{\alpha 5} = 0;$$

$$-\mathrm{i}\bar{\alpha}r\boldsymbol{B}_\alpha = r\boldsymbol{H}_1^*\boldsymbol{B}_\alpha - \frac{\mathrm{d}}{\mathrm{d}r}(r\boldsymbol{H}_2^*\boldsymbol{B}_\alpha) + \frac{\mathrm{d}^2}{\mathrm{d}r^2}(r\boldsymbol{H}_3^*\boldsymbol{B}_\alpha); \tag{3.8}$$

$$r = 1: \qquad B_{\alpha 2} = B_{\alpha 4} = B_{\alpha 6} = 0.$$

In (3.8), '$*$' denotes an adjoint matrix; the overbar indicates a complex conjugate. The problem (3.7) is a regular direct problem of the normal mode analysis; it was considered in §2. The problem (3.8) is an adjoint one.

The following orthogonality relation is valid:

$$\langle \boldsymbol{A}_\alpha, \boldsymbol{B}_\gamma\rangle \equiv \int_0^1 r(\boldsymbol{A}_\alpha, \boldsymbol{B}_\gamma)\,\mathrm{d}r = \int_0^1 r\sum_{j=1}^{6} A_{\alpha j}\bar{B}_{\gamma j}\,\mathrm{d}r = \delta_{\alpha\gamma}, \tag{3.9}$$

where $\delta_{\alpha\gamma}$ is the Kronecker symbol. From (3.3) and (3.8) we obtain the relation

$$\langle \boldsymbol{A}_v, \boldsymbol{B}_\alpha\rangle \mathrm{i}(\alpha_v - \alpha) - (\boldsymbol{H}_2\boldsymbol{A}_v, \boldsymbol{B}_\alpha)_{r=1} = 0, \tag{3.10}$$

which will be used in the analysis of the integral (3.6). The boundary conditions for the numerical solution of the adjoint problem are described in Appendix B.

3.3. *The receptivity problem solution*

We assume that the biorthogonal eigenfunction system $\{\boldsymbol{A}_\alpha, \boldsymbol{B}_\alpha\}$ is a complete one; thus solution (3.6) may be written as the sum

$$\boldsymbol{A} = \frac{1}{2\pi}\int_{-\infty}^{\infty} \boldsymbol{A}_v\mathrm{e}^{\mathrm{i}\alpha_v z}\,\mathrm{d}\alpha_v = \sum_\alpha C_\alpha\boldsymbol{A}_\alpha\mathrm{e}^{\mathrm{i}\alpha z}. \tag{3.11}$$

Application of the orthogonality relationship (3.9) and (3.10) gives the amplitude coefficient C_α:

$$C_\alpha = \langle \boldsymbol{A}, \boldsymbol{B}_\alpha\rangle \mathrm{e}^{-\mathrm{i}\alpha z} = \frac{1}{2\pi}\int_{-\infty}^{\infty} \langle \boldsymbol{A}_v, \boldsymbol{B}_\alpha\rangle\,\mathrm{e}^{\mathrm{i}(\alpha_v-\alpha)z}\,\mathrm{d}\alpha_v$$

$$= \frac{1}{2\pi\mathrm{i}}\int_{-\infty}^{\infty} \frac{(\boldsymbol{H}_2\boldsymbol{A}_v, \boldsymbol{B}_\alpha)_{r=1}}{\alpha_v - \alpha}\,\mathrm{e}^{\mathrm{i}(\alpha_v-\alpha)z}\,\mathrm{d}\alpha_v. \tag{3.12}$$

For $z > 0$ we can use an integration path in the complex plane α_v as shown in figure

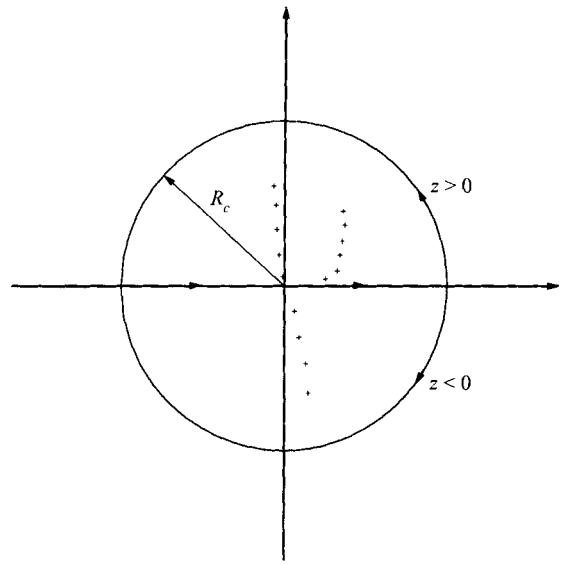

FIGURE 4. Sketch of the integral path in the complex plane α_r for $z > 0$ and $z < 0$.

4 when the radius of the circle R_c tends to infinity; and the input of the mode α from the upper semi-plane is equal to

$$C_\alpha = -\varrho(\alpha)B_{\alpha 3}(r = 1), \tag{3.13}$$

where the explicit form of the matrix $\boldsymbol{H}_2$ is taken into account. The final result for the longitudinal velocity disturbance component is written as

$$w(t, r, \vartheta, z) = -\mathrm{Re}\left\{ \sum_\alpha \varrho(\alpha)B_{\alpha 3}(r = 1)\, \mathrm{e}^{\mathrm{i}\alpha z + \mathrm{i}n\vartheta - \mathrm{i}\omega t} A_{\alpha 3}(r) \right\}. \tag{3.14}$$

3.4. *Numerical results*

We introduce the receptivity coefficient RC_α:

$$RC_\alpha = \varrho(\alpha)B_{\alpha 3}(r = 1). \tag{3.15}$$

The coefficient depends on normalization of the eigenfunction A_α. Since in our normalization the maximum longitudinal velocity amplitude was chosen equal to 1, the coefficient gives the initial amplitude and the phase of the velocity component. Its value depends on the shape function $f(z)$. As an example of the shape function $f(z)$ in (3.1) we choose a step function, thus $\varrho(\alpha) = 2\sin(\alpha d/2)/\alpha$. In our numerical examples, the function $\varrho(\alpha) \approx d$ for $d \leqslant 0.5$ and the results referred to d are almost independent of the slot width in the range of d.

For the case of the azimuthal index $n = 0$, we took into consideration 24 least-stable meridional eigenmodes. The result of the receptivity coefficient calculation for this mode, without taking into account the acoustic mode input, is shown in figure 5.

The two values labelled A and B correspond to the eigenvalues A and B shown in figure 1. The other meridional modes are numbered in accordance with the value of α_i. The result illustrates that the least-stable eigenmodes are not excited by the forcing flow through the wall and the maximum excitation exists for eigenmode 17 with the eigenvalue $\alpha = 1.641 + \mathrm{i}2.416$. The real and imaginary parts of the longitudinal

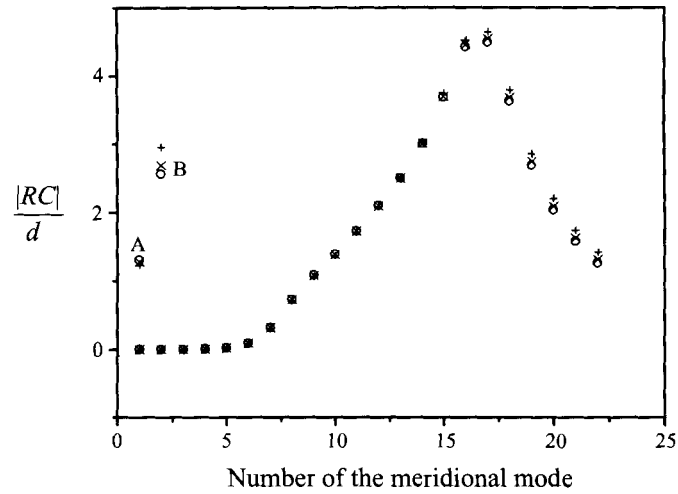

FIGURE 5. Receptivity coefficient. $n = 0$. $d = 0.1(\circ); 0.3(\times); 0.5(+)$.

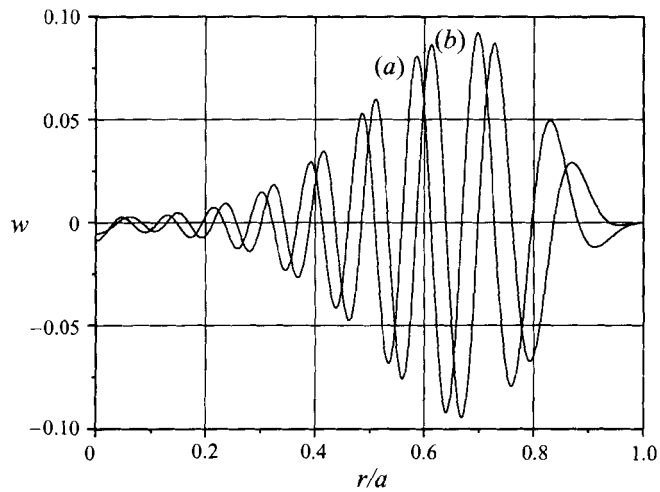

FIGURE 6. The longitudinal velocity component of meridional eigenmode 17 ($n = 0$). (*a*) Re(w); (*b*) Im(w).

velocity component w of eigenmode 17 are shown in figure 6. The maximum of the velocity disturbance is close to the wall, while the least-stable eigenmode (figure 2) has its maximum at the centreline.

The receptivity coefficient for the azimuthal index $n = 1$ is shown in figure 7(*a*). There are four values A,B,C and D corresponding to the distant eigenvalues in figure 3. The modes corresponding to the first family have a bigger response than those from the second family.

The result for RC, when the azimuthal index $n = 2$, is shown in figure 7(*b*). The most efficient excitation exists for eigenmode 9 of the first family at $\alpha = 1.604 + i0.824$.

The receptivity coefficient for the azimuthal index $n = 3$ is demonstrated in figure 7(*c*). The maximum value of the coefficient corresponds to eigenmode 10 of the first family at $\alpha = 1.639 + i1.08$. The results show that the most efficient eigenmodes

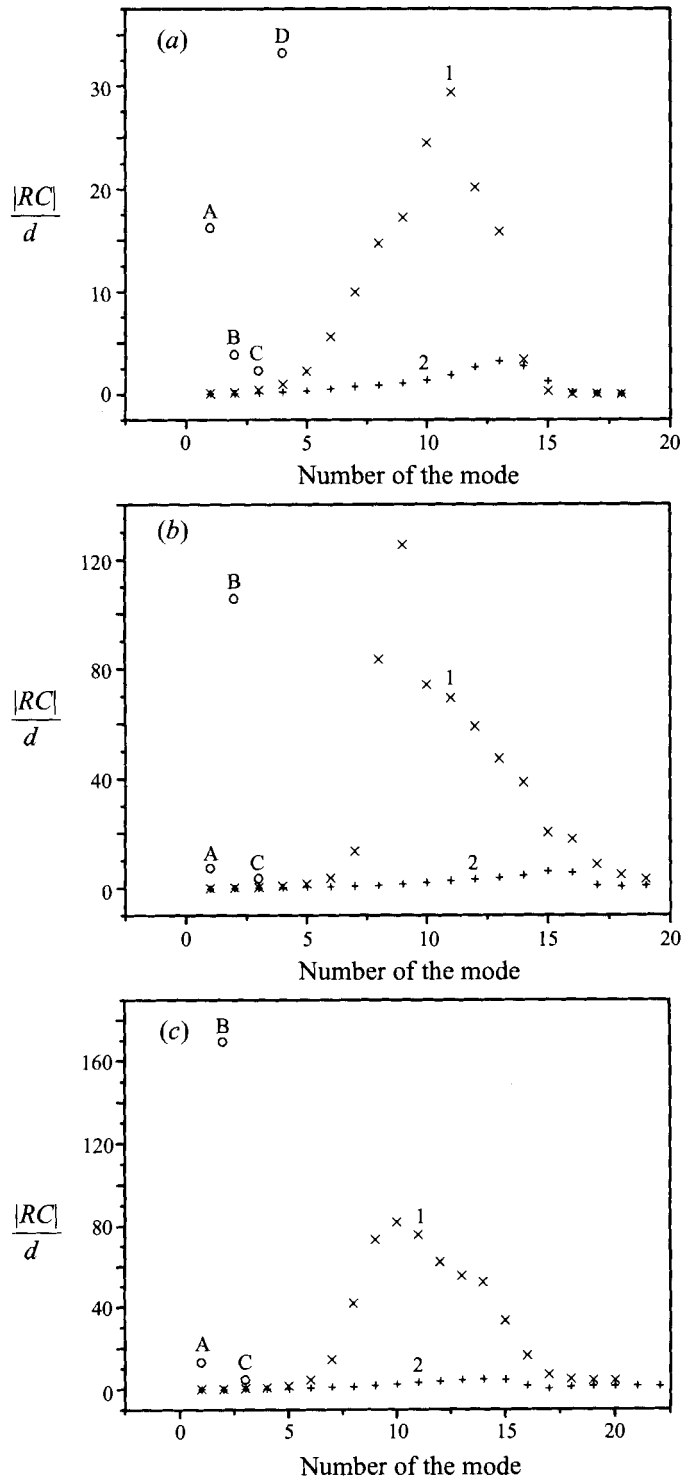

FIGURE 7. Receptivity coefficient when (*a*) $n = 1$, (*b*) $n = 2$, (*c*) $n = 3$. $d = 0.1$.

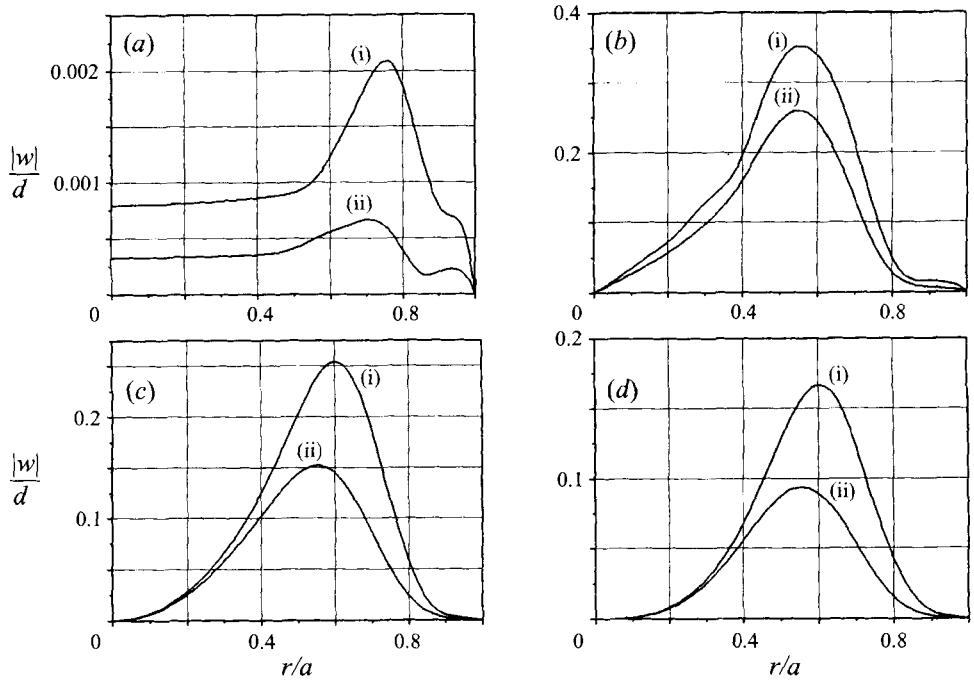

FIGURE 8. Longitudinal velocity component of the forced disturbance.
(i) $z = 6.6$; (ii) $z = 8.6$. (*a*) $n = 0$; (*b*) $n = 1$; (*c*) $n = 2$; (*d*) $n = 3$.

excited in a pipe flow have the maximum velocity disturbance relatively close to a wall, while the least-stable eigenmodes have the maximum close to the centreline.

Far from the slot the disturbance field may be described by a finite number of least-stable eigenmodes, because the others will decay significantly; and the number of eigenmodes that must be taken into account depends on the distance from the slot and on their initial amplitudes. To imitate an experimental observation in a pipe flow, we considered two stations: $z = 6.6$ and $z = 8.6$. The results for $n = 0$ (without input from the acoustic mode), 1, 2 and 3 are shown in figure 8: 24 least-stable meridional eigenmodes were taken into account for $n = 0$; 40 eigenmodes were taken for $n = 1$; 42 for $n = 2$ and 45 for $n = 3$ respectively.

Acoustic mode excitation depends on an instantaneous mass flux through a slot. If the mass flux is equal to zero, the 'acoustic' amplitude is also equal to zero. In our example given for the step function, the instantaneous mass flux is not equal to zero and the acoustic mode is excited by a source having an amplitude much bigger than the amplitude of the hydrodynamic modes. The 'acoustic' mode distribution at $z = 6.6$ is shown in figure 9.

4. Summary

The global eigenvalue problem for pipe Poiseuille flow was treated by using the collocation method based on the Chebyshev polynomial expansion. The numerical method is identical to the method of Khorrami *et al.* (1989).

Receptivity analysis carried out for forcing through a wall slot shows that the least-stable eigenmodes cannot be excited efficiently. There are some more stable eigenmodes that have an efficient response to the forcing. A Physical explanation is

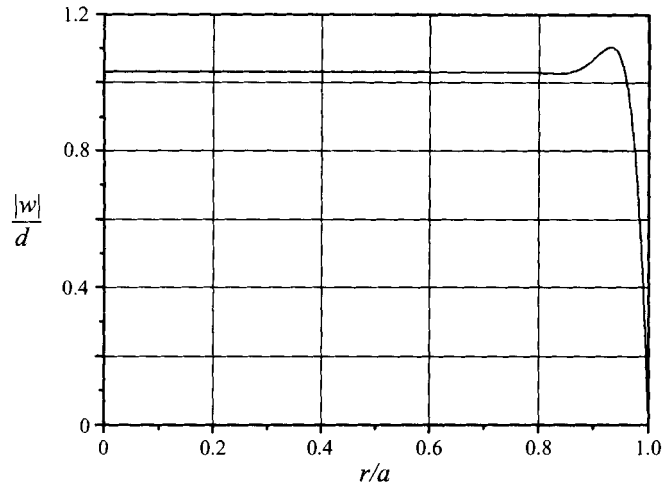

FIGURE 9. Acoustic mode response at $z = 6.6$.

that blow–suction through a wall cannot strongly disturb the flow at the centre, so, for the most part, it generates disturbances localized near a wall. The more stable disturbances are localized closer to the wall. The more stable a mode, the more oscillating a character it has across a pipe. We can expect that there is a mode with the most effective response to blow-suction through a wall.

Because the more stable axisymmetric and non-axisymmetric eigenmodes have the maximum longitudinal velocity component close to the wall, we should observe a shift of the maximum towards to the centre during the downstream development of all the perturbations. This result explains the non-similar character of the disturbances observed by Leite (1959) in different locations along a pipe. We want to emphasize that we deal with a number of eigenmode excitations and a general picture and a decaying rate could not be explained in terms of one eigenmode at a reasonable distance from a slot.

The numerical example does not allow us to illustrate possibility of transient growth when blow–suction through a wall is used. First of all, we considered only the step function for velocity distribution in a slot. Secondly, we could not consider the perturbations which are closer to the slot. To consider the perturbations in the vicinity of the slot we need to take into account a lot of damping eigenmodes, so the numerical procedure becomes too complicated.

Further theoretical and experimental investigations of pipe flow at the linear stage are necessary. We suppose that any future experimental work should be done simultaneously with an appropriate analysis of the flow receptivity with respect to the method of generation used. For example, blow–suction periodic with respect to time through a wall may be used. It will be necessary to measure the velocity disturbances downstream of a slot by using facilities similar to those used by Cohen & Wygnanski (1987) for disturbances in an axisymmetric jet. They measured the phase-locked velocity disturbances as a function of time by using eight hot-wires at different locations across a jet. The measurements allowed the decomposition of a signal to be carried out in order to obtain the disturbance distribution corresponding to different azimuthal indices. The main difficulty in an experiment with blow–suction through the pipe wall will be associated with the measurement of the velocity profile at the edge of the slot. Based on investigations in boundary layers (Ivanov & Kachanov

1994), we can suggest that some kind of a vibrator placed on a wall would be more preferable. In such a case, the method of the receptivity problem solution will be the same but the boundary conditions (3.1) will change their form as in the boundary layer case (Tumin & Fedorov 1984).

The author is grateful to Professor I. Wygnanski for attracting the author's interest to the problem of the Poiseuille pipe flow. Also, the author greatly appreciates the meetings with Professor E. Reshotko, who supported the author's attention to the receptivity problem and pointed out many publications dealing with the pipe flow problem. The author also appreciates the useful discussions of the results with Professor E. Kerschen and Professor H. Fasel. The author thanks Dr G. Zilman for the useful advice on computational aspects of the problem.

The work was supported by the Guastela scholarship from the Rashi foundation.

Appendix A. Non-zero elements of matrices H_1, H_2 and H_3

$$H_1^{12} = 1;$$

$$H_1^{21} = \frac{(n^2+1)}{r^2} - i\omega Re; \quad H_1^{22} = Re\, W(r); \quad H_1^{25} = \frac{2in}{r^2};$$

$$H_1^{31} = -\frac{1}{r}; \quad H_1^{35} = -\frac{in}{r};$$

$$H_1^{41} = \frac{W(r)}{r} - \frac{dW}{dr}; \quad H_1^{42} = -\frac{1}{Rer}; \quad H_1^{43} = i\omega - \frac{n^2}{Rer^2};$$

$$H_1^{45} = \frac{inW(r)}{r}; \quad H_1^{46} = -\frac{in}{Rer}; \quad H_1^{56} = 1;$$

$$H_1^{61} = -\frac{2in}{r^2}; \quad H_1^{64} = \frac{inRe}{r}; \quad H_1^{65} = -i\omega Re + \frac{(n^2+1)}{r^2}; \quad H_1^{66} = ReW(r);$$

$$H_2^{21} = -\frac{1}{r}; \quad H_2^{24} = Re; \quad H_2^{31} = -1;$$

$$H_2^{41} = W(r); \quad H_2^{42} = -\frac{1}{Re}; \quad H_2^{43} = \frac{1}{Rer};$$

$$H_2^{65} = -\frac{1}{r}; \quad H_3^{21} = -1; \quad H_3^{43} = \frac{1}{Re}; \quad H_3^{65} = -1.$$

Appendix B. Boundary conditions for the numerical solution of the adjoint problem

The numerical method used for the adjoint problem is, at the same time, the spectral collocation method. For the numerical procedure we have to formulate the boundary conditions at $r = 1$ and $r \to 0$.

The boundary conditions at $r = 1$ are written in (3.8). For the numerical treatment we have to use some additional conditions that follow from the equations. From the sixth equation of the system (3.8) we obtain

$$B_{\alpha 5} = 0. \tag{B 1}$$

From the second equation we have at $r = 1$

$$B_{\alpha 1} + \frac{1}{Re}\frac{dB_{\alpha 4}}{dr} = 0. \tag{B 2}$$

The other boundary condition at $r = 1$ follows from the fourth equation of the system (3.8):

$$\frac{dB_{\alpha 2}}{dr} = 0. \tag{B 3}$$

Thus, we formulate the following boundary conditions at $r = 1$:

$$\left.\begin{aligned} r = 1: \quad & B_{\alpha 2} = B_{\alpha 4} = B_{\alpha 5} = B_{\alpha 6} = 0; \\ & \frac{dB_{\alpha 2}}{dr} = 0; \\ & B_{\alpha 1} + \frac{1}{Re}\frac{dB_{\alpha 4}}{dr} = 0. \end{aligned}\right\} \tag{B 4}$$

At $r \to 0$ the solution must be finite. If we consider the axisymmetric mode ($n = 0$), we obtain $B_{\alpha 2} = 0$ from the fourth equation. From the third equation it follows that $B'_{\alpha 4} = 0$, and from the fifth equation we find $B_{\alpha 6} = 0$. Hence, the sixth and the second equations give $B_{\alpha 5} = 0$ and $B_{\alpha 1} = 0$ respectively. From the first equation we have

$$-\frac{3}{2}\frac{d^2 B_{\alpha 2}}{dr^2} + \frac{dB_{\alpha 3}}{dr} = 0. \tag{B 5}$$

Finally, we formulate the boundary conditions for the axisymmetric mode at $r \to 0$:

$$\left.\begin{aligned} n = 0; \quad r \to 0: \quad & B_{\alpha 1} = B_{\alpha 2} = B_{\alpha 5} = B_{\alpha 6} = 0; \\ & -\frac{3}{2}\frac{d^2 B_{\alpha 2}}{dr^2} + \frac{dB_{\alpha 3}}{dr} = 0, \\ & \frac{dB_{\alpha 4}}{dr} = 0. \end{aligned}\right\} \tag{B 6}$$

From the sixth equation for the indexes $n = \pm 1$ we determine that $B_{\alpha 4}$ must be equal to 0; from the fifth equation we have at $r \to 0$: $B_{\alpha 6} - inB_{\alpha 2} = 0$. The first and the fourth equations give two conditions: $B'_{\alpha 2} = B'_{\alpha 6} = 0$; and from the fifth equation it follows that $B_{\alpha 3}$ must be equal to zero. If we subtract the second equation from the sixth equation with the factor in, we find that $inB_{\alpha 5} + B_{\alpha 1} = 0$ at $r \to 0$. To summarize the boundary conditions we can present them as

$$\left.\begin{aligned} n = \pm 1 \quad r \to 0: \quad & B_{\alpha 3} = B_{\alpha 4} = 0; \\ & \frac{dB_{\alpha 2}}{dr} = \frac{dB_{\alpha 6}}{dr} = 0; \\ & B_{\alpha 6} - inB_{\alpha 2} = 0; \\ & B_{\alpha 1} + inB_{\alpha 5} = 0. \end{aligned}\right\} \tag{B 7}$$

From the first, third and fifth equations for the indices $|n| \geqslant 2$ we obtain that $B_{\alpha 2} = B_{\alpha 4} = B_{\alpha 6} = 0$ at $r \to 0$. From the sixth equation it follows that $B_{\alpha 5} = 0$, and the second equation also gives $B_{\alpha 1} + Re^{-1}B'_{\alpha 4} = 0$. The fourth and fifth equations give $B_{\alpha 3}$ equal to zero. Thus, the boundary conditions are written as

$$\left.\begin{aligned} |n| \geqslant 2 \quad r \to 0: \quad & B_{\alpha 2} = B_{\alpha 3} = B_{\alpha 4} = B_{\alpha 5} = B_{\alpha 6} = 0; \\ & B_{\alpha 1} + \frac{1}{Re}\frac{dB_{\alpha 4}}{dr} = 0. \end{aligned}\right\} \tag{B 8}$$

REFERENCES

ASHPIS, D. E. & RESHOTKO, E. 1990 The vibrating ribbon problem revisited. *J. Fluid Mech.* **213**, 513–547.

BERGSTRÖM, L. 1992 Initial algebraic growth of small angular dependent disturbances in pipe Poiseuille flow. *Stud. Appl. Maths* **87**, 61–79.

BERGSTRÖM, L. 1993*a* Optimal growth of small disturbances in pipe Poiseuille flow. *Phys. Fluids* A **5**, 2710–2719.

BERGSTRÖM, L. 1993*b* Evolution of laminar disturbances in pipe Poiseuille flow. *Eur. J. Mech.* B/Fluids **12**, 749–768.

BOBERG, L. & BROSA, U. 1988 Onset of turbulence in a pipe. *Z. Naturforsch.* **43 a**, 697–726

BRAMLEY, J. S. 1986 The calculation of eigenvalues for the stationary perturbation of symmetrical pipe Poiseuille flow. *J. Comput. Phys.* **64**, 258–265.

CHOUDHARY, M. 1993 Roughness-induced generation of crossflow vortices in three-dimensional boundary layers. *NASA-CR* 4505.

COHEN, J. & WYGNANSKI, I. 1987 The evolution of instabilities in the axisymmetric jet. Part 1. The linear growth of disturbances near the nozzle. *J. Fluid Mech.* **176**, 191–219.

CORCOS, G. M. & SELLARS, J. R. 1959 On the stability of fully developed flow in a pipe. *J. Fluid Mech.* **5**, 97–112.

DARBYSHIRE, A. G. & MULLIN, T. 1995 Transition to turbulence in constant-mass-flux pipe flow. *J. Fluid Mech.* **289**, 83–114.

DRAZIN, P. G. & REID, W. H. 1981 *Hydrodynamic Stability*. Cambrige University Press.

FEDOROV, A. V. 1984 Excitation of Tollmien-Schlichting waves in a boundary layer by a periodic external source located on the body surface. *Fluid Dyn.* **19**, 888–893 (from Russian).

FOX, J. A., LESSEN, M. & BHAT, W. V. 1968 Experimental investigation of the stability of Hagen-Poiseuille flow. *Phys. Fluids* **11**, 1–4.

GARG, V. K. & ROULEAU, W. T. 1972 Linear spatial stability of pipe Poiseuille flow. *J. Fluid Mech.* **54**, 113–127.

GASTER, M. 1965 On the generation of spatially growing waves in a boundary layer. *J. Fluid Mech.* **22**, 433–441.

GILL, A. E. 1965 On the behaviour of small disturbances to Poiseuille flow in a circular pipe. *J. Fluid Mech.* **21**, 145–172.

GOLDSTEIN, M. E. & HULTGREN, L. S. 1989 Boundary layer receptivity to long wave free-stream disturbances. *Ann. Rev. Fluid Mech.* **21**, 137–166.

GUSTAVSSON, L. H. 1989 Direct resonance of nonaxisymmetric disturbances in pipe flow. *Stud. Appl. Maths* **80**, 95–108.

IVANOV, A. V. & KACHANOV, YU. S. 1994 Excitation and development of spatial packets of instability waves in a three-dimensional boundary layer. *Thermophys. Aeromech. Russian Acad. Sci.* **1**, No. 4, 287–305.

KASKEL, A. 1961 Experimental study of the stability of pipe flow. II. Development of disturbance generator. *Jet Propulsion Laboratory Tech. Rep.* 32–138. Pasadena, California.

KHORRAMI, M. R., MALIK, M. R. & ASH, R. L. 1989 Application of spectral collocation techniques to the stability of swirling flows. *J. Comput. Phys.* **81**, 206–229.

LEITE, R. J. 1959 An experimental investigation of the stability of Poiseuille flow. *J. Fluid Mech.* **5**, 81–97.

LESSEN, M., SADLER, S. G. & LIU, T. Y. 1968 Stability of pipe Poiseuille flow. *Phys. Fluids* **11**, 1404–1409.

LIANG, F. P. & RESHOTKO, E. 1991 An inviscid stability analysis of unbounded supersonic mixing layer flows. *EMAE/TR* 90 - 199, Case Western Reserve University, Cleveland.

LIN, C. C. 1955 *The Theory of Hydrodynamic Stability*. Cambrige University Press.

MORKOVIN, M. V. 1969 Critical evaluation of transition from laminar to turbulent shear layers with emphasis on hypersonically traveling bodies. *AFF DL-TR*-68-149, Air Force Flight Dynamics Lab., Wright-Patherson AFB, Ohio.

MORKOVIN, M. V. & RESHOTKO, E. 1989 Dialogue on progress and issues in stability and transition research. In *Laminar-Turbulent Transition, IUTAM Symp., Toulouse* (ed. D. Arnal & R. Michel), pp. 1–29. Springer.

PEKERIS, C. L. 1948 Stability of the laminar flow through a straight pipe of circular cross section

to infinitesimal disturbance which are symmetrical about the axis of the pipe. *Proc. US Natl Acad. Sci.* **34**, 285–295.

PHILLIPS, T. N. & ROBERTS, G. W. 1993 The treatment of spurious pressure modes in spectral incompressible flow calculations. *J. Comput. Phys.* **105**, 150–164.

PRETSCH, J. 1941 Über die Stabilität der Laminarströmung in einem geraden Rohr mit Kreisförmigem Querschmitt. *Z. Angew. Math. Mech.* **21**, 204–217.

RESHOTKO, E. 1958 Experimental study of the stability of pipe flow. I. Establishment of an axially symmetric Poiseuille flow. *Jet Propulsion Laboratory, Progress Rep.* 20-364, Pasadena, California.

RESHOTKO, E. 1976 Boundary-layer stability and transition. *Ann. Rev. Fluid Mech.* **8**, 311–349.

REYNOLDS, O. 1883 An experimental investigation of the circumstances which determine whether the motion of water shall be direct or sinuous, and of the law of resistance in parallel channels. *Phil. Trans. R. Soc. Lond.* **174**, 935–982.

SALWEN, H., COTTON, F. W. & GROSCH, C. E. 1980 Linear stability of Poiseuille flow in a circular pipe. *J. Fluid Mech.* **98**, 273–284.

SALWEN, H. & GROSCH, C. E. 1972 The stability of Poiseuille flow in a pipe of a circular cross-section. *J. Fluid Mech.* **54**, 93–112.

SCHMID, P. J. & HENNINGSON, D. S. 1994 Optimal energy density growth in Hagen-Poiseuille flow. *J. Fluid Mech.* **277**, 197–225.

SEXL, TH. 1927*a* Zur Stabilitätsfrage der Poiseuilleschen und Couetteschen Strömung. *Ann. Physik* **83**, 835–848.

SEXL, TH. 1927*b* Über dreidimensionale Störungen der Poiseuilleschen Strömung. *Ann. Physik* **84**, 807–822.

TATSUMI, T. 1952 Stability of the laminar inlet-flow prior to the formation of Poiseuille regime, Part II. *J. Phys. Soc. Japan* **7**, 495–502.

TUMIN, A. M. & FEDOROV, A. V. 1984 Instability wave excitation by a localized vibrator in the boundary layer. *J. Appl. Mech. Tech. Phys.* **25**, 867–873 (from Russian).

WYGNANSKI, I. & CHAMPAGNE, F. H. 1973 On transition in a pipe flow. *J. Fluid Mech.* **59**, 281–335.

ZHIGULEV, V. N. & TUMIN, A. M. 1987 *Origin of Turbulence.* Novosibirsk, Nauka (in Russian).